Framework Doping of Iron in Tunnel Structure Cryptomelane

Jun Cai,[†] Jia Liu,[‡] William S. Willis,[†,‡] and Steven L. Suib*[,†,‡,§]

Department of Chemistry, U-60, Institute of Materials Science, and Department of Chemical Engineering, University of Connecticut, Storrs, Connecticut 06269-3060

Received December 29, 2000. Revised Manuscript Received May 8, 2001

A framework doping method was proposed to dope transition-metal iron ions into the framework instead of the tunnels of 2 × 2 tunnel structure manganese octahedral molecular sieve cryptomelane. Iron was first doped into the MnO_6 octahedra layers of layered structure birnessite, which served as a synthetic precursor for tunnel structure cryptomelane. Iron-doped cryptomelane was obtained by the thermal transformation of iron-doped birnessite. The effects of temperature and the amount of iron doping on the thermal transformation from birnessite to cryptomelane were also studied. Iron was evenly doped into the framework without producing other phases if iron doping was less than 10% of the total manganese. Hematite phases appeared if iron doping reached 16% of the total manganese. A doping limit of iron was observed for tunnel structure cryptomelane. X-ray photoelectron spectroscopy and electron paramagnetic resonance were used to analyze the local chemical environment of manganese and iron in cryptomelane, suggesting iron was doped into the framework instead of the tunnels. Iron doping had a great impact on the microstructure and properties of cryptomelane. The amount of K^+ in tunnels, the average oxidation state of manganese, and the vibrational frequency of the Mn−O band increased with the amount of iron doping. The thermal stability of cryptomelane was improved by iron doping. The prepared cryptomelane had a large number of basic sites, and the strength of these sites increased with increasing amounts of iron doping.

Introduction

Octahedral molecular sieves (OMS) have been widely used or proposed for possible use in catalysis, batteries, separations, chemical sensors, and other applications.[1−6] These materials usually have open framework structures and large surface areas. They can be synthesized from transition metals such as Mn and Fe. Manganese octahedral molecular sieves are mixed-valence manganese oxides having tunnels that are made from edge-shared and corner-shared MnO_6 octahedra.[7] The electrochemical interest of mixed valency in biology, chemistry, and physics gives OMS a unique role in scientific and industrial research.

Cryptomelane is a manganese octahedral molecular sieve consisting of 4.6 Å × 4.6 Å tunnels due to double chains of edge-sharing MnO_6 octahedra that corner share to form square tunnels that are two octahedra on a side.[8−11,13b,c] The unit cell of cryptomelane proposed by Ramsdell is tetragonal with $a = 9.84$ Å and $c = 2.85$ Å.[8] Manganese in cryptomelane are in the Mn^{4+} and Mn^{3+} oxidation states and in octahedral sites.[12,13] Potassium ions are in the tunnels to stabilize the tunnel structure and can be partly ion-exchanged with other cations.[14,15]

Substitution in framework sites of manganese octahedral molecular sieves by other metals is possible by doping the original reactant solutions with cations.[7] Because the physical and chemical properties of doped manganese octahedral molecular sieves are greatly influenced by the type, the amount, and the location of the doping ions, the properties of doped materials are significantly different from those of the undoped ones.[5,7] Some work has been done to dope different metal cations into manganese octahedral molecular sieves such as synthetic todorokite (OMS-1) and synthetic cryptomelane (OMS-2),[5,16−18,21] but only work of doping cations into tunnels of OMS has been reported, especially in

* To whom correspondence should be addressed.
† Department of Chemistry, U-60.
‡ Institute of Materials Science.
§ Department of Chemical Engineering.

(1) Bish, R. G.; Post, J. E. *Geol. Soc. Am. Abstr. Programs* **1984**, *16*, 446.
(2) Shen, Y. F.; Zerger, R. P.; DeGuzman, R. N.; Suib, S. L.; McCurdy, L.; Potter, D. I.; O'Young, C. L. *Science* **1993**, *260*, 511.
(3) Bach, B.; Periera-Ramos, J. P.; Baffier, N.; Messina, R. *Electrochim. Acta* **1991**, *36*, 1595.
(4) Euler, K. J.; Mueller-Helsa, H. J. *Power Sources* **1979**, *4*, 77.
(5) (a) Post, J. E.; Bish, D. L. *Am. Mineral.* **1988**, *73*, 861. (b) Shen, Y. F.; Suib, S. L.; O'Young, C. L. *J. Am. Chem. Soc.* **1994**, *116*, 11020.
(6) DeGuzman, R. N.; Awaluddin, A.; Shen, Y. F.; Tian, Z. R.; Suib, S. L.; Ching, S.; O'Young, C. L. *Chem. Mater.* **1995**, *7*, 1286.
(7) Suib, S. L. *Curr. Opin. Solid State Mater. Sci.* **1998**, *3*, 63.
(8) Ramsdell, A. *Am. Mineral.* **1942**, *27*, 611.
(9) Bystrom, A.; Bystrom, A. M. *Acta Crystallogr.* **1950**, *3*, 146.
(10) Post, J. E.; Burnham, C. W. *Am. Mineral.* **1986**, *71*, 1178.
(11) Giovanoli, R.; Faller, M. *Chimia* **1989**, *43*, 54.
(12) Turner, S.; Buseck, P. R. *Science* **1981**, *212*, 1024.
(13) (a) Feng, Q.; Kanoh, H.; Miyai, Y.; Ooi, K. *Chem. Mater.* **1995**, *7*, 148. (b) Post, J. E.; Von Dreele, R. B.; Buseck, P. R. *Acta Crystallogr.* **1982**, *B38*, 1056. (c) Post, J. E. *Proc. Natl. Acad. Sci. U.S.A.* **1999**, *96*, 3447.
(14) Tsuji, M.; Abe, M. *Solvent Extr. Ion Exch.* **1984**, *2*, 253.
(15) Giovanoli, R.; Balmer, B. *Chimia* **1981**, *35*, 53.
(16) Nicolas-Tolentino, E.; Tian, Z. R.; Zhou, H.; Xia, G. G.; Suib, S. L. *Chem. Mater.* **1999**, *11*, 1733.

10.1021/cm0014233 CCC: $20.00
Published on Web 06/16/2001

synthetic todorokite. Todorokite has 6.9 Å × 6.9 Å tunnels formed by triple chains of edge-sharing MnO_6 octahedra that corner share to form large square tunnels that are three octahedra on a side.[5] Doping metals of about 10−20% manganese can be doped into todorokite.[5,21] However, the total doping in cryptomelane is very limited, typically in the range of 0.01−0.5%.[16−18] A typical method for preparing cryptomelane is to oxidize Mn^{2+} using $KMnO_4$ in acidic solutions with refluxing.[7,17] Dopants are added into the reactant solution prior to refluxing. Because first-row transition-metal ions have great solubility in acidic solutions, it is very difficult to incorporate these ions into the framework of cryptomelane using this preparation method. They are more likely to stay in solution or in the tunnels of cryptomelane as ions than to be incorporated into the framework.[17] Therefore, only the tunnels of OMS materials easily accommodate cation dopants, and a larger tunnel size facilitates the doping. The size differences between todorokite and cryptomelane tunnels probably account for the fact that significantly more transition-metal ions can be doped into todorokite than into cryptomelane structures. The framework doping of transition-metal ions into cryptomelane requires a different synthesis approach.

In this paper, a new method of doping transition-metal ions into the framework of cryptomelane was attempted. A transition-metal ion-doped precursor, birnessite, was prepared first. Birnessite (OL-1) is an octahedral layered manganese oxide that can be synthesized by the oxidation of Mn^{2+} in basic solutions. OL-1 has a two-dimensional layered structure that consists of edge-shared MnO_6 octahedra, with cations and water molecules occupying the interlayer region.[19] The interlayer distance in birnessite is typically 7.1 Å. Transition-metal ions were added prior to the oxidation and were incorporated into the MnO_6 layers. Cations other than K^+ in the interlayer region were all exchanged to K^+ by ion exchange. Then, the doped birnessite was calcined to 800 °C to form framework-doped cryptomelane. Because crystallographic studies have shown that the formation of tunneled manganese oxides from birnessite precursors is due to a collapse of the layer framework around the interstitial cations,[20,37] the doped cations would be in the framework instead of in the tunnels of cryptomelane. Iron was chosen as the dopant in this study because of the similar sizes, charges, and coordination tendencies to form octahedra with oxygen atoms and manganese ions. The amount of doping was varied to study the doping capacity of cryptomelane. The structures and the physical and chemical properties of the framework-doped cryptomelane were also studied to understand the effects of framework doping in cryptomelane.

Experimental Section

Synthesis of Iron-Doped Birnessite and Cryptomelane. About 7.5 g of $MnCl_2 \cdot 4H_2O$ was dissolved in 50 mL of deionized water. $FeCl_3$ was added into the solution with Fe/Mn atomic ratios of 0, 1/20, 1/10, and 1/5 at room temperature under agitation. Air was bubbled into the Fe^{3+} and Mn^{2+} solutions at a flow rate of 16 L/min. An 80 mL solution containing 20 g of NaOH was then added dropwise into the solution for 30 min. After 6 h of reaction, the product was filtered, washed, and then transferred to a 250 mL solution of 18.6 g of KCl for ion exchange at room temperature under stirring for 12 h. The ion-exchanged product was filtered and washed three times with 1 L of deionized water. The K-birnessite was dried in air at 65 °C for 24 h and then placed in a furnace to calcine stepwise in air at 200, 400, 600, and 800 °C for 2 h, respectively. Small amounts of products were taken out at each step to study the crystal phases.

Characterization. X-ray diffraction (XRD) experiments were carried out on a Scintag XDS 2000 diffractometer with a Cu Kα radiation source.

X-ray photoelectron spectroscopy (XPS) was done on a Leybold-Heraeus model 3000 spectrometer upgraded with a SPECS EA10MCD energy analyzer. Cryptomelane powder samples were pressed into indium foil to minimize charging.

Electron paramagnetic resonance (EPR) measurements were done on a Bruker ESP 300 X-band spectrometer. Samples were diluted with diamagnetic silica, evacuated, and sealed in a quartz tube. The operational conditions are as follows: 9.424 GHz frequency, 10.18 mW power, 100 kHz modulation frequency, and 110 K temperature.

Inductively coupled plasma atomic emission spectroscopy (ICP-AES) analyses were done on a Perkin-Elmer 7−40 instrument. Powder samples of cryptomelane were weighed and dissolved in a 1% HCl solution.

Scanning electron microscope (SEM) photographs were taken on an AMRAY 1810 SEM. Chemical compositions of samples were determined by energy-dispersive X-ray analysis (EDAX) on a Philips PV9800 EDAX spectrometer with a Super Quant program.

The average oxidation state (AOS) of manganese was obtained by a potentiometric titration method.[22−24] Cryptomelane was reduced by concentrated HCl to Mn^{2+} and then was titrated to Mn^{3+} in a $Na_2S_2O_7$ solution using a $KMnO_4$ standard solution to get the total amount of manganese. Then, the AOS of manganese was determined by reducing cryptomelane to Mn^{2+} with $(NH_3)_2Fe(SO_4)_2$ and backtitrating the excess Fe^{2+} with the $KMnO_4$ standard solution.

(17) DeGuzman, R. N.; Shen, Y. F.; Neth, E. J.; Suib, S. L.; O'Young, C. L.; Levine, S.; Newsam, J. M. *Chem. Mater.* **1994**, *6*, 815.
(18) Zhou, H.; Wang, J. Y.; Chen, X.; O'Young, C. L.; Suib, S. L. *Micropor. Mesopor. Mater.* **1998**, *21*, 315.
(19) Post, J. E.; Veblen, D. R. *Am. Mineral.* **1990**, *75*, 477.
(20) Ching, S.; Petrovay, D. J.; Jorgensen, M. L.; Suib, S. L. *Inorg. Chem.* **1997**, *36*, 883.
(21) Luo, J.; Zhang, Q. H.; Huang, A.; Giraldo, O.; Suib, S. L. *Inorg. Chem.* **1999**, *38*, 6106.
(22) Glover, D.; Schumm, B., Jr.; Kozowa, A. *Handbook of Manganese Dioxides Battery Grade*; International Battery Materials Association: 1989, Cleveland, OH.
(23) Brock, S. L.; Sanabria, M.; Suib, S. L.; Urban, V.; Thiyagarajan, P.; Potter, D. I. *J. Phys. Chem. B* **1999**, *103*, 7416.
(24) Murray, J. W.; Balistieri, L. S.; Paul, B. *Geochim. Cosmochim. Acta* **1984**, *48*, 1237.
(25) Luo, J.; Suib, S. L. *J. Phys. Chem. B* **1997**, *101*, 10403.
(26) Golden, D. C.; Dixon, J. B.; Chen, C. C. *Clays Clay Miner.* **1986**, *34*, 511.
(27) Wagner, C. D.; Riggs, W. M.; Davis, L. E.; Moulder, J. F.; Muilenberg, G. E. *Handbook of X-ray Photoelectron Spectroscopy*; Perkin-Elmer Corp.: New York, 1979.
(28) Drago, R. S. *Physical Methods in Chemistry*; W. B. Saunders Co.: Philadelphia, PA, 1977; p 348.
(29) Wakehan, S.; Carpenter, R. *Chem. Geol.* **1974**, *13*, 39.
(30) (a) Potter, R. M.; Rossman, G. R. *Am. Mineral.* **1979**, *64*, 1199. (b) Park, S. H.; McClain, S.; Tian, Z. R.; Suib, S. L.; Karwacki, C. *Chem. Mater.* **1997**, *9*, 176.
(31) Zhang, Q.; Luo, J.; Vileno, E.; Suib, S. L. *Chem. Mater.* **1997**, *9*, 2090.
(32) Cornell, R. M.; Schwertmann, U. *The Iron Oxides*; VCH Publishers: New York, 1996; pp 127−135.
(33) Nyquist, R. A.; Kagel, R. O. *Infrared Spectra of Inorganic Compounds*; Academic Press: New York, 1971; pp 216−219.
(34) Corma, A. *Chem. Rev.* **1995**, *95*, 559.
(35) Hatori, H. *Chem. Rev.* **1995**, *95*, 537.
(36) Lide, D. R. *CRC Handbook of Chemistry and Physics*, 73rd ed.; CRC Press: Boca Raton, FL, 1992; pp 8−12.
(37) Chen, C. C.; Golden, D. C.; Dixon, J. B. *Clays Clay Miner.* **1986**, *34*, 565.

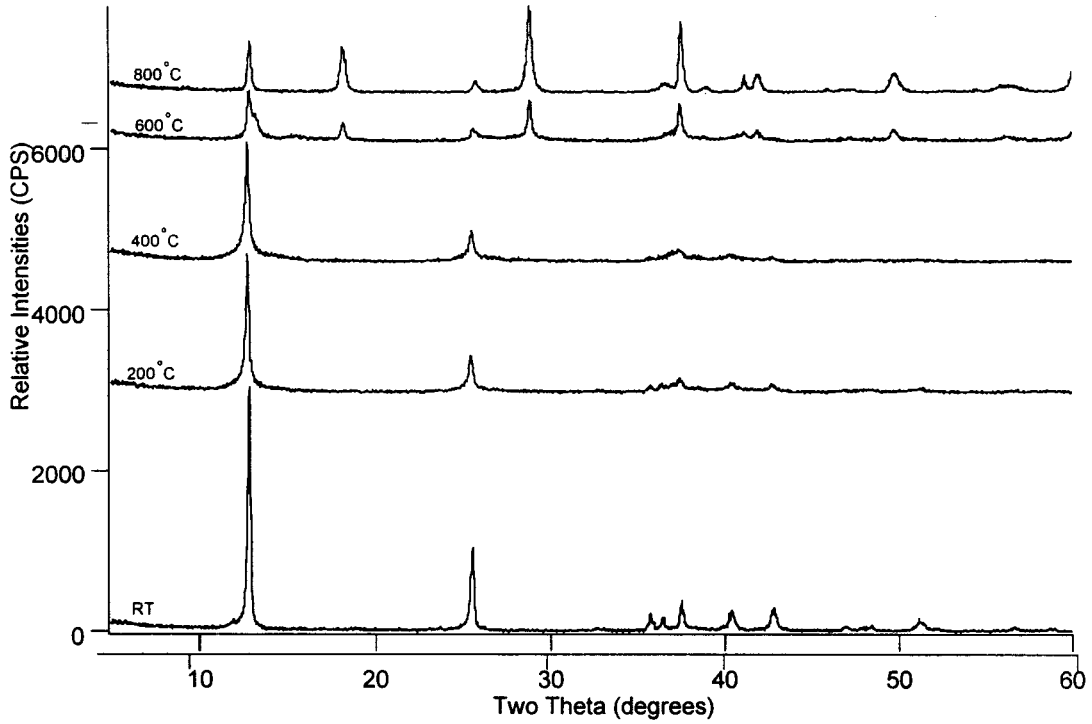

Figure 1. XRD patterns of birnessite after heating in air at different temperatures.

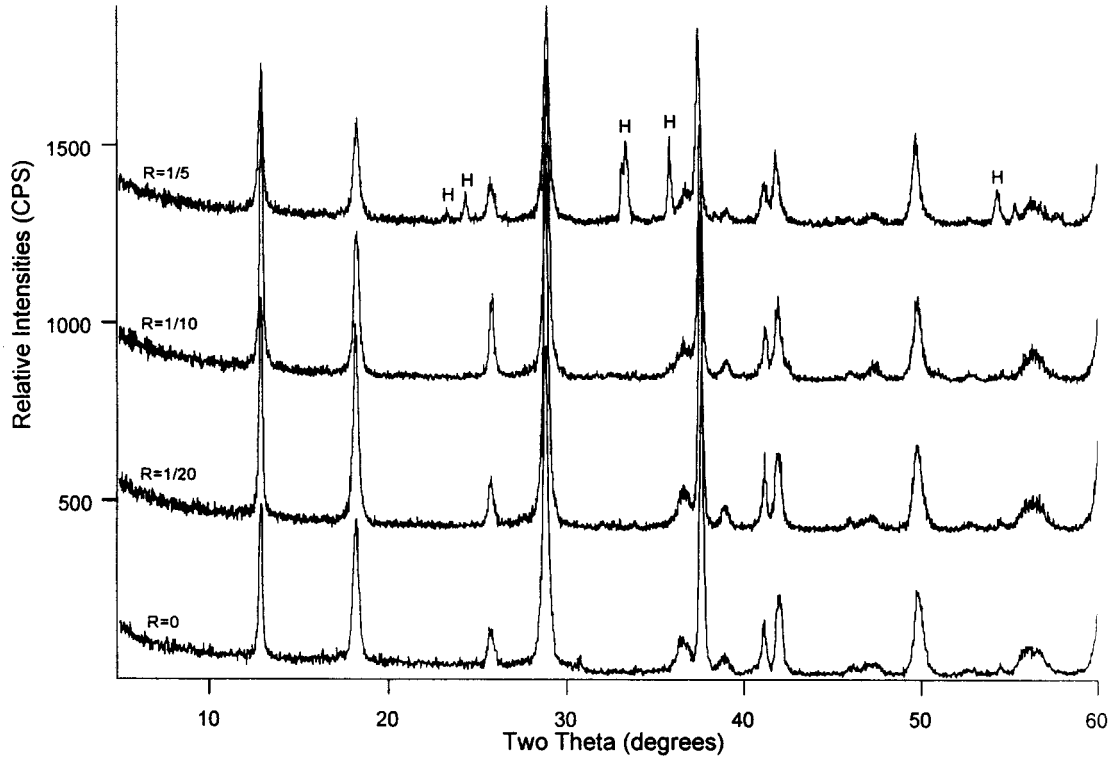

Figure 2. XRD patterns of cryptomelane formed after heat treatment (H: hematite).

Fourier transform infrared (FTIR) spectra were taken on a Nicolet Magna-IR system 750 FTIR spectrometer with an MCT-B detector and a KBr beam splitter. The black cryptomelane powder was diluted to 1 wt % in a KBr pellet.

Thermogravimetric analyses (TGA) were performed on a Hi-Res TGA 2950 model thermogravimetric analyzer. Differential scanning calorimetry (DSC) experiments were done on a DSC 2900 model DSC. The temperature ramp for TGA and DSC was 10 °C/min, and the carrier gas was nitrogen.

Temperature-programmed desorption combined with a mass spectrometer (TPD-MS) was done with a furnace and a MKS−UTI PPT quadrupole residual MS gas analyzer. The thermal properties were studied first. After being purged by He for 6 h, cryptomelane samples were heated at a rate of 10 °C/min to 700 °C. The downstream gas was analyzed by the MS system. The acidic and basic properties of cryptomelane were studied as follows. Cryptomelane samples were pretreated at 700 °C in He for 2 h and cooled to room temperature. Then samples were exposed to 1% CO_2/He or NH_3/He for 2 h. Samples adsorbed with CO_2 or NH_3 were evacuated and purged with He for 12 h. Samples were then heated at 10 °C/min to 700 °C, and the downstream gas was analyzed.

Table 1. Binding Energies (eV) of Fe 2p, Mn 2p, and O 1s Peaks from Doped OMS-2 Samples

	sample					
	$R = 0$		$R = 1/10$		$R = 1/5$	
peak	BE (eV)	Δ_{BE} (eV)	BE (eV)	Δ_{BE} (eV)	BE (eV)	Δ_{BE} (eV)
Fe $2p_{1/2}$	*a*	*a*	724.33		724.44	
Fe $2p_{3/2}$	*a*	*a*	710.90	13.43	710.79	13.65
Mn $2p_{1/2}$	653.74		653.82		653.78	
Mn $2p_{3/2}$	642.11	11.63	642.05	11.77	642.01	11.77
O 1s	529.40		529.40		529.41	

[a] Not observed.

Results

Synthesis of Fe−Cryptomelane. Birnessite was prepared by the air oxidation of $Mn(OH)_2$ in a basic solution. Because birnessite was the precursor for preparing cryptomelane, a well-crystallized birnessite was essential. The amount of Fe doping was varied to study its effect on the formation and crystalline growth of birnessite. Fe/Mn ratios of 0, 1/20, 1/10, and 1/5 were used. From the XRD patterns, no significant difference could be found in the structure of birnessite. Fe was incorporated well in birnessite without causing apparent disorder of the structure.

According to work done by Golden et al.,[26] birnessite with only K^+ cations in the interlayers produced pure cryptomelane upon thermal transformation. Birnessite with cations other than K^+ gave other phases such as hausmannite and bixbyite. Therefore, K^+ ion exchange was done to saturate the interlayers of birnessite with K^+ ions and remove other exchangeable cations. The products formed when heating K^+-saturated birnessite at different temperatures are shown in Figure 1. K^+-saturated birnessite was stable to 400 °C. Cryptomelane peaks first appeared at 600 °C and were more intense and better separated at 800 °C. These data suggest that cryptomelane was formed after heating.

However, the amount of iron doping played a prominent role in producing the final product, as illustrated by the XRD patterns of products formed after heating at 800 °C in Figure 2. No other phase except cryptomelane was present in the XRD patterns after the heat treatment if the Fe/Mn ratio was less than 1/10. When the Fe/Mn ratio was 1/5, hematite (Fe_2O_3) coexisted with cryptomelane. Excessive iron doping in the Fe/Mn ratio of the 1/5 sample resulted in the formation of hematite.

XPS. XPS analyses were carried out to obtain information on the local chemical environments of manganese and iron in cryptomelane from the variations in binding energies, or chemical shifts, of the photoelectron lines. Because chemical shifts are very uniform among the photoelectron lines of an element, line separations rarely vary by more than 0.2 eV.[27] A change in the separation of photoelectron lines can suggest a change in the local environment. Binding energies of Fe 2p, Mn 2p, and O 1s peaks of Fe-doped cryptomelane are listed in Table 1.

The iron $2p_{1/2}$ and $2p_{3/2}$ peaks occurred at about 724 and 710 eV, respectively, for all iron-doped cryptomelane samples. The two binding energies were very close to those of Fe_2O_3 Fe 2p peaks. However, the separation of the iron $2p_{1/2}$ and $2p_{3/2}$ peaks Δ_{BE} increased from 13.43 to 13.65 eV when the iron doping ratio was increased from 1/10 to 1/5. This was a significant change because the difference was greater than 0.2 eV, suggesting that there was a local environment change for iron. This change could be due to the formation of Fe_2O_3 because of the excessive doping of iron in cryptomelane. The binding energies for Mn $2p_{1/2}$ and Mn $2p_{3/2}$ peaks of all samples were about 653 and 642 eV, which are very close to those of MnO_2 Mn 2p peaks. The line separation for Mn $2p_{1/2}$ and Mn $2p_{3/2}$ peaks Δ_{BE} was

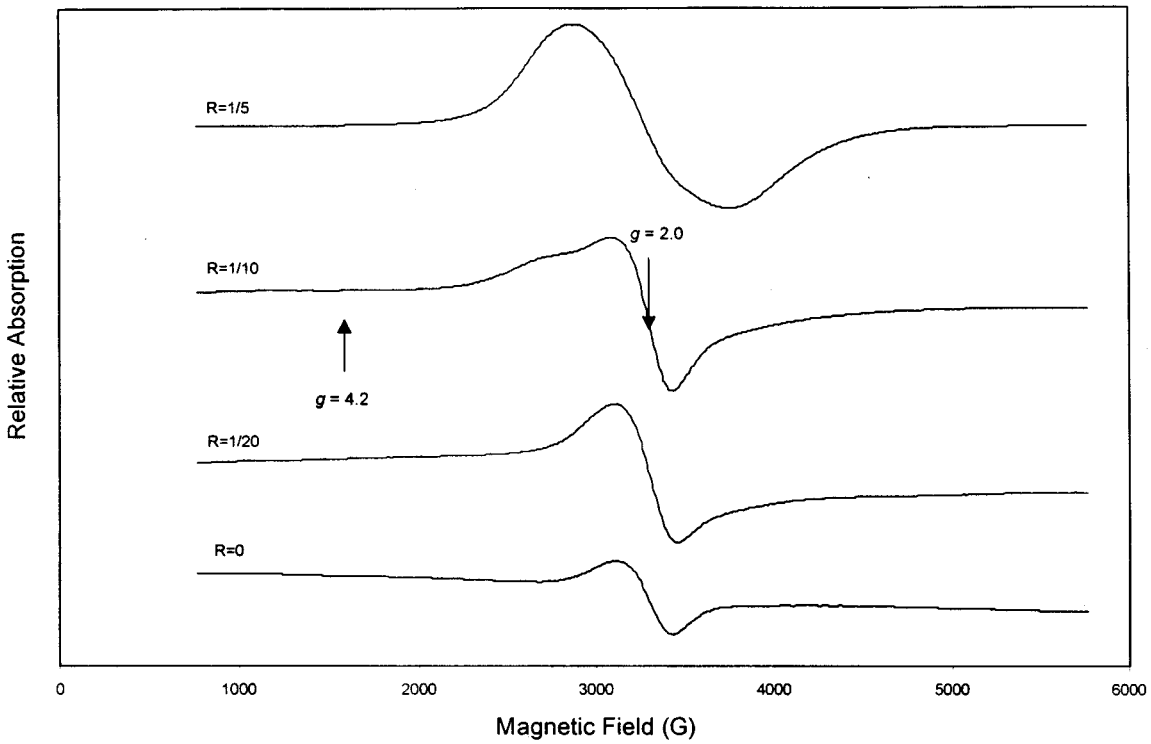

Figure 3. X-band EPR spectra of cryptomelane with different amounts of iron doping at 110 K.

Table 2. Compositions of K, Fe, and Mn in Doped OMS-2 Samples, As Determined by ICP-AES and EDAX, and AOS of Mn[a]

sample	elemental analysis			
	ICP-AES		EDAX	
ratio Fe/Mn	ratio Fe/Mn	ratio K/(Mn + Fe)	ratio Fe/Mn	AOS of Mn
0	0.001	0.206	0	3.67
1/20	0.050	0.238	0.055	3.76
1/10	0.103	0.245	0.102	3.80
1/5	0.158	0.170	0.184	3.61

[a] Ratios shown are atomic ratios.

11.63 eV for pure cryptomelane but was 11.77 eV for both iron-doped cryptomelane samples, which was not as significant because it was less than 0.2 eV. The binding energy of O 1s remained unchanged at 529.4 eV even when the amount of iron doping was changed.

EPR Measurements. The EPR measurements were used to study the chemical environments of Mn and Fe in cryptomelane.[28,29] The EPR spectra of cryptomelane samples are shown in Figure 3. These spectra are characterized by a broad symmetric resonance with a *g* value of 2.0 and with intensities and peak-to-peak line widths increasing with increasing amounts of iron doping. No hyperfine and no other resonances were found after the iron doping, implying that no new coordination structure other than octahedra was created.

Elemental Analyses and AOS of Manganese. Compositions of K, Fe, and Mn in cryptomelane samples and the AOS of manganese are listed in Table 2.

The atomic ratios of Fe to Mn of cryptomelane samples determined by ICP-AES and by EDAX matched the initial ratios of reactants added. The Fe/Mn atomic ratio for the 1/5 sample determined by EDAX (0.184) was considerably larger than the ratio determined by ICP-AES (0.158), suggesting that some Fe might go into interlayer sites in this excessively doped sample. The K/Mn ratio for cryptomelane was analyzed by ICP-AES as well. This ratio increased when iron doping was below 10.3% of the manganese but decreased dramatically when iron doping reached 15.8%.

The AOSs of manganese ranged from 3.6 to 3.8, depending on the amount of iron doping. If the iron doping was less than 1/5 of the manganese in cryptomelane, the AOS of manganese increased gradually with increasing amounts of doping, reaching the highest value of 3.80 when iron doping was 1/10 of the manganese. The AOS dropped significantly to 3.61 when the doping ratio was 1/5 of manganese, which was even less than that for pure cryptomelane (3.67). Therefore, iron doping, in fact, increased the AOS of manganese in cryptomelane if no excess iron was doped. Excessive iron doping caused a decrease in the AOS of manganese in cryptomelane.

Infrared (IR) Spectroscopy. IR spectra of cryptomelane samples are shown in Figure 4. Water was not observed in the IR spectra.

The undoped cryptomelane had a weak band at 1398 cm^{-1}, and the iron-doped material had a broad band at 1455 cm^{-1} in IR spectra, which have not been observed in mineral cryptomelane, synthetic cryptomelane prepared in acidic solutions, or hematite.[30a,31,33] Because cryptomelane was prepared in a basic solution by air oxidation using this method, CO_2 was inevitably absorbed. Bands in the 1400−1460 cm^{-1} region for cryptomelane can be attributed to a C−O stretching vibration of carboxylate groups that are metal dependent.[30b] The one at 1398 cm^{-1} for pure cryptomelane was very weak and was subsequently overlapped by a broader band centered at 1455 cm^{-1} after Fe was doped into the

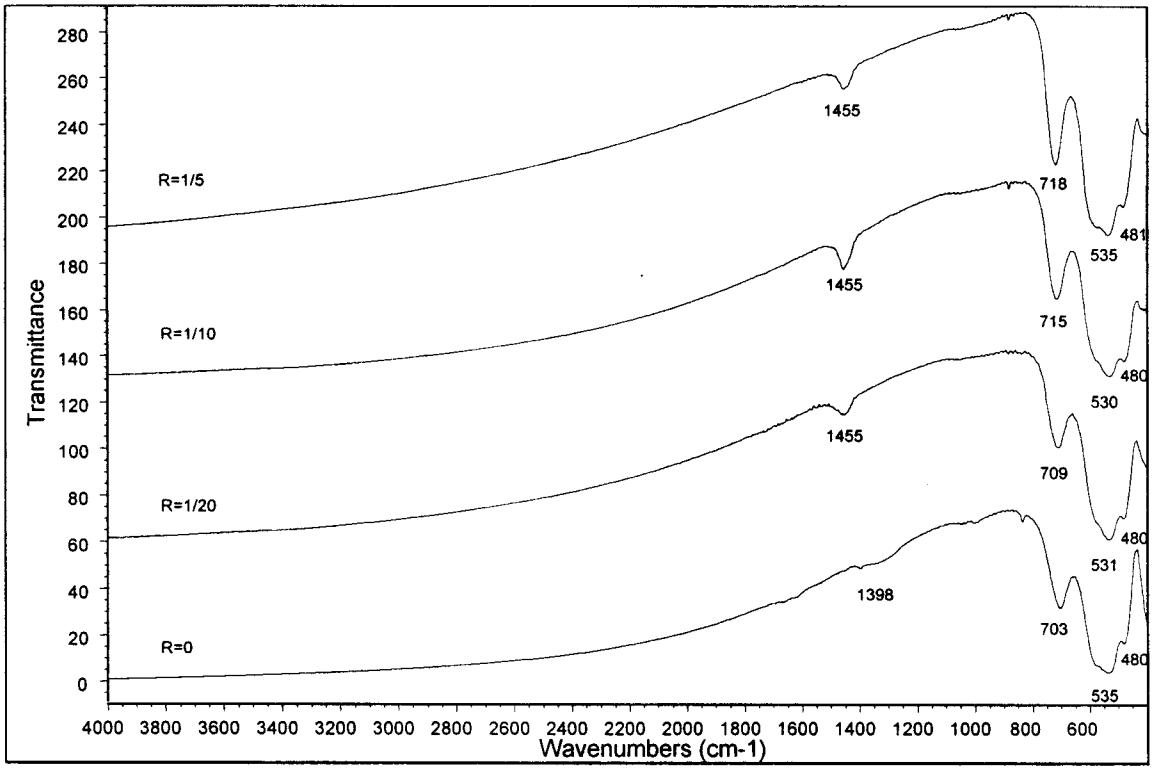

Figure 4. IR spectra of cryptomelane with different amounts of iron doping.

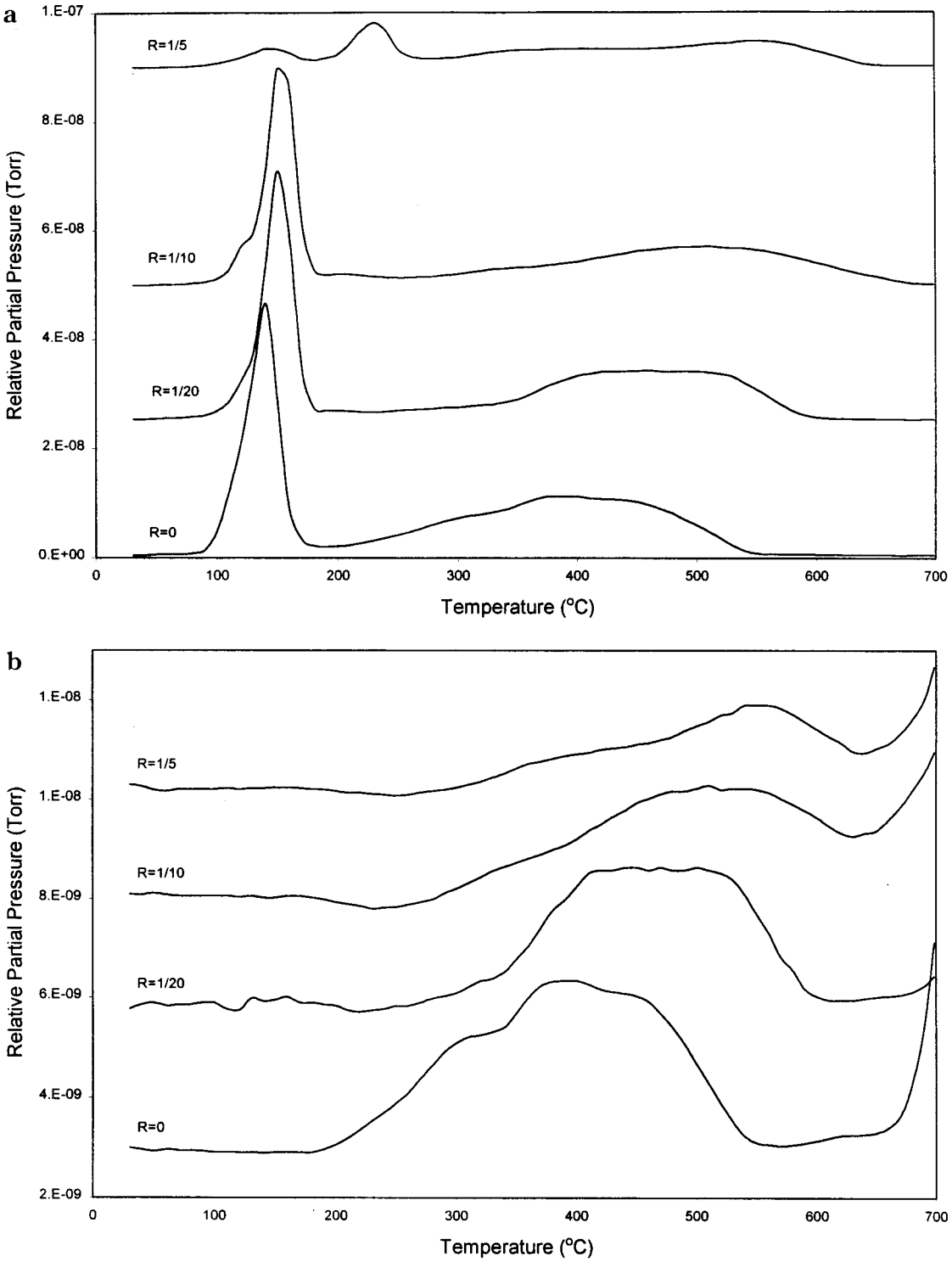

Figure 5. TPD plots of cryptomelane samples in a helium atmosphere: (a) CO_2 peaks; (b) O_2 peaks.

framework. The appearance of this broad band could be due to interaction between iron and carboxylate groups.

The three bands in the region 450−750 cm^{-1} were attributed to Mn−O and Fe−O vibrations.[30a,31,32] When the amount of iron doping gradually increased, the positions of bands at 480 and 535 cm^{-1} remained about the same but the vibrational frequency of the band at 703 cm^{-1} increased gradually at the same time. The frequency was 703, 709, 715, and 718 cm^{-1} for cryptomelane samples with 0, 1/20, 1/10, and 1/5 iron to manganese molar ratios of iron doping.

Thermal Analyses. TPD was done to study gases adsorbed by cryptomelane. CO_2 and O_2 were the main products of the TPD, and their TPD plots are shown in Figure 5. Thermal properties of cryptomelane are shown by the TGA and DSC data in Figures 6 and 7.

Carbon dioxide was desorbed from cryptomelane at different temperatures depending on the strength of adsorption. Weakly adsorbed or bonded CO_2 was desorbed at low temperatures, and medium and strongly adsorbed or bonded CO_2 were desorbed at higher temperatures. One sharp and one very broad CO_2 peak were observed in the TPD in temperature ranges of 100−200

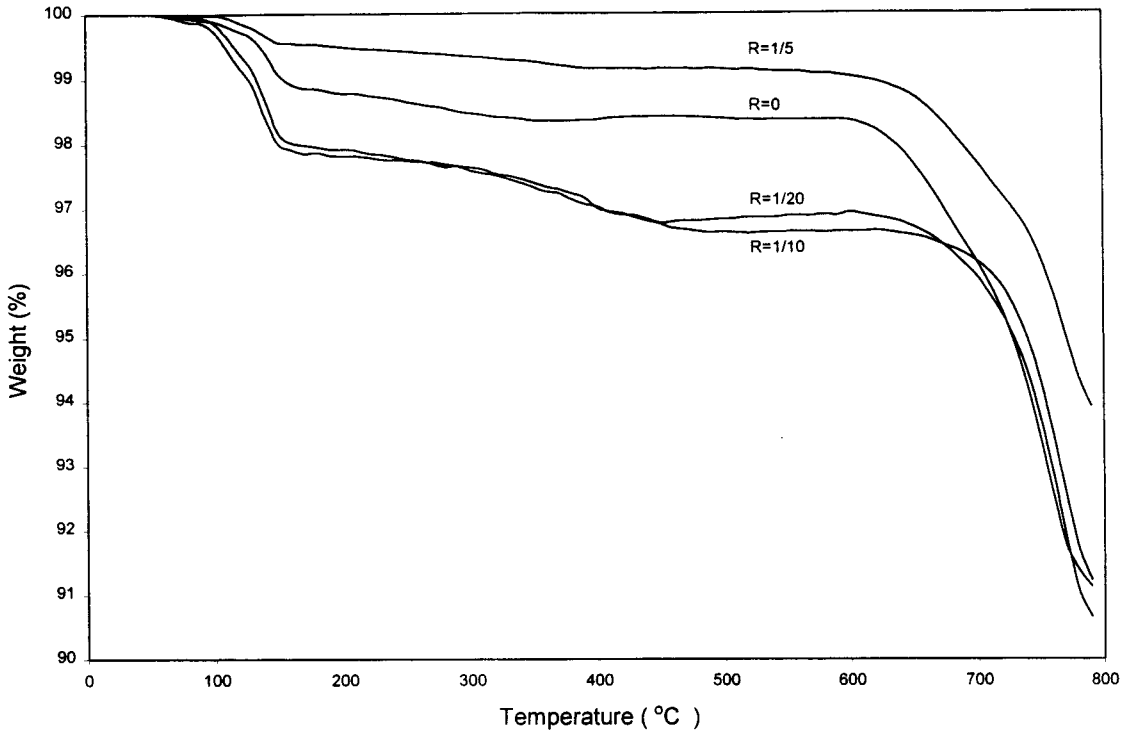

Figure 6. TGA of cryptomelane samples in a nitrogen atmosphere.

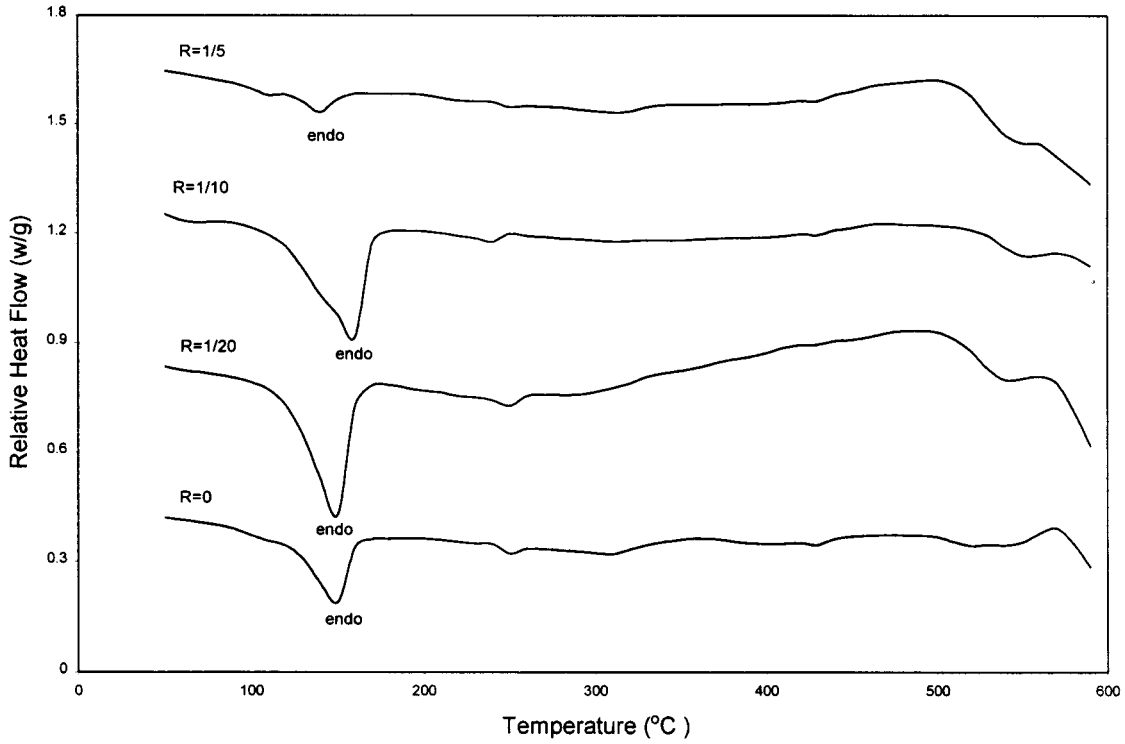

Figure 7. DSC of cryptomelane samples in a nitrogen atmosphere.

and 300−600 °C for cryptomelane samples with iron doping of no more than 1/10 of the total manganese content. These two peaks shifted slightly to higher temperatures when more iron was doped into the framework, suggesting that iron doping improved the strength of the adsorption. When the doping ratio was 1/5, one extra peak at 240 °C appeared. The appearance of this extra peak could be due to desorption of CO_2 adsorbed by hematite.

In the TPD plots of O_2, almost no O_2 was released before 200 °C. There was a broad peak of O_2 between 200 and 650 °C, shifting to higher temperatures when more iron was doped into cryptomelane. O_2 released at this stage can be due to oxygen adsorbed on the surface and in the framework of cryptomelane. The existence of iron in the framework may help retain oxygen and stabilize the tunnel structure.

TGA profiles of cryptomelane samples in N_2 showed almost no weight loss before 100 °C. This was consistent with IR data in Figure 4, which exhibited no water bands. The first weight loss occurred at 100−200 °C, ranging from 0.5% to 2.2%. Cryptomelane samples with

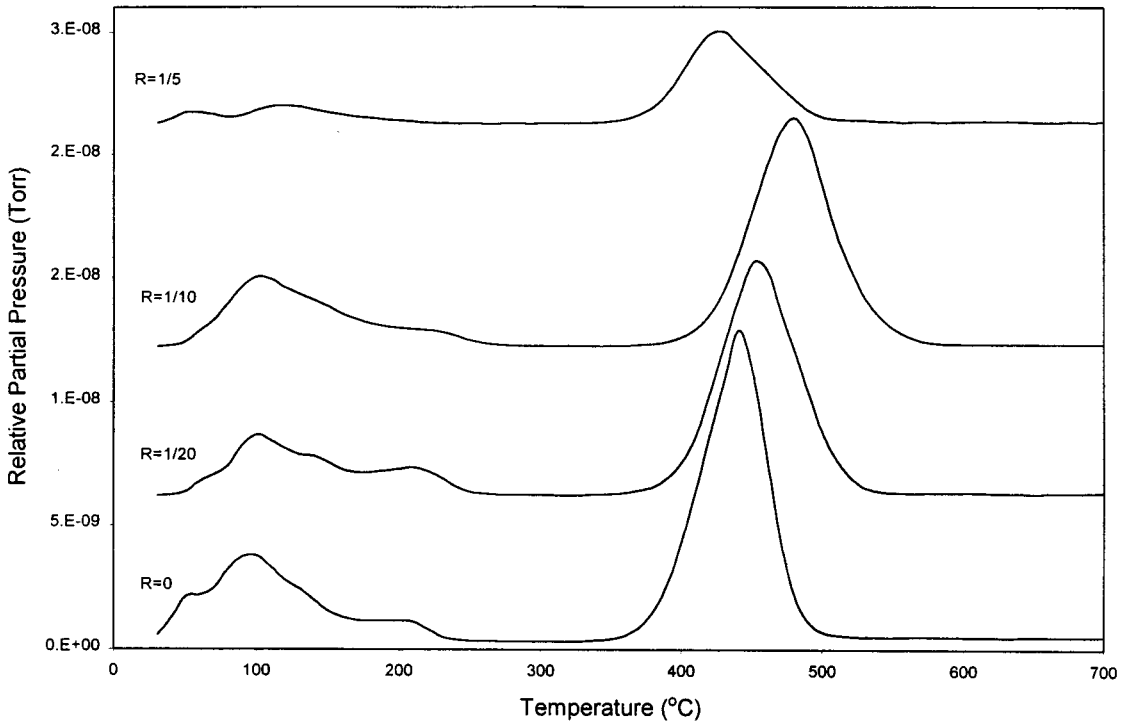

Figure 8. TPD plots of CO_2 adsorbed on high-temperature pretreated cryptomelane.

higher iron doping had more weight loss, but the one with excessive iron doping had the least weight loss. This loss corresponded to the loss of CO_2 in the TPD plots. No other loss such as H_2O or O_2 was observed in TPD plots in this temperature region. The greater the amount of doped iron, the more CO_2 was attracted to cryptomelane.

DSC measurements on cryptomelane exhibited a prominent endothermic peak at 100−200 °C. Referring to TPD and TGA data, this peak could be due to the release of a large amount of CO_2. Heat flow was in proportion to the amount of CO_2 released in this range. No significant heat flow changes could be detected above 200 °C.

Acidity and Basicity Measurements. Cryptomelane was preheated to 700 °C in helium for 2 h to remove any adsorbed species such as CO_2 and O_2 from the surface in order to reveal acidic and basic sites. After cooling, cryptomelane was exposed to NH_3 or CO_2 for excessive adsorption. Physically adsorbed NH_3 or CO_2 was then removed by prolonged evacuation and helium purging before TPD was conducted.

NH_3 TPD is used to measure the acidity of solids.[34] In this measurement only very weak NH_3 signals can be detected with a large signal-to-noise ratio. These data suggest that there are almost no acidic sites in these synthesized cryptomelane samples.

CO_2 TPD is used to measure the number and strength of basic sites. The amount and strength of the basic sites are reflected in the TPD plots from the peak area and the desorption temperature of CO_2.[35] Figure 8 shows the CO_2 TPD plots of cryptomelane. There are two peaks in the CO_2 TPD plots: one is at low temperature from room temperature to 250 °C; the other is at high temperature from 350 to 550 °C. CO_2 desorbed at low temperature was adsorbed on weak basic sites. All samples had about the same number of weak basic sites except for the material with a ratio of 1/5. CO_2 desorbed at high temperature was adsorbed on strong basic sites. There were more strong basic sites than weak sites. The strength of the strong basic sites increased when more iron was doped into the framework but decreased when excessive iron was introduced.

Discussion

A successful doping of cryptomelane depends on the successful synthesis and doping of birnessite. The fact that iron doping up to 15.8% of the total manganese did not significantly change the XRD pattern of birnessite indicated that Fe^{3+} ions were well incorporated into the birnessite framework without apparently disrupting the layered structure. The similar sizes, charges, and coordination tendencies of manganese and iron cations might have contributed to the success of iron doping in MnO_6 octahedral layers. Ionic radii of octahedral Mn^{3+}, Fe^{3+}, and Mn^{4+} in crystals are 0.58, 0.55, and 0.53 Å, respectively.[36] Fe^{3+} can substitute either for Mn^{3+} or Mn^{4+} without causing much structural disorder and serious charge imbalance. K^+ played an important role in the formation of cryptomelane upon thermal transformation.[26] Cryptomelane may be regarded as having two sets of parallel octahedral sheets intersecting each other at near 90°.[37] Arrhenius and Tsai proposed that the transformation of birnessite to cryptomelane takes place by pillaring of the MnO_6 octahedra between birnessite octahedral sheets.[38] The pillars eventually coalesce to form a perpendicular set of octahedral sheets in the cryptomelane structure. The large K^+ ions may act as spacers between octahedral sheets and help prevent the birnessite layers from collapsing during the heating process.[38] Because Fe was already doped into the layers of synthetic birnessite with K^+ in the inter-

(38) Arrhenius, G. O.; Tsai, A. G. *SIO Ref. Series* **1981**, *81−28*, 1.

layer region, after thermal transformation, Fe remained in the framework of cryptomelane with K^+ in the tunnels.

XPS measurements of iron and manganese shed light on the changes in the local chemical environment when the amount of iron doping was varied. The significant change in the line separation of Fe $2p_{1/2}$ and Fe $2p_{3/2}$ peaks Δ_{BE} showed that there was a change in the local environment of iron. In the 1/10 doping ratio sample, analyzed iron had the same local environment as iron in the framework, which was surrounded by MnO_6 octahedra. However, in the 1/5 doping ratio sample, hematite, in which iron was surrounded by FeO_6 octahedra, had a different local chemical environment from iron in the framework. Two totally different local chemical environments could account for the significant change in the Fe $2p_{1/2}$ and Fe $2p_{3/2}$ peak separation. For manganese, there was also a difference in the line separation of Mn 2p peaks Δ_{BE} between the undoped and iron-doped cryptomelane samples. Because synthetic cryptomelane was the matrix and no more than 16% of manganese iron could be doped into the framework, the influence of Fe on Mn was much weaker and the change in the local chemical environment of manganese was not as significant. Therefore, the change in $2p_{1/2}$ and $2p_{3/2}$ peak separation for Mn was not as large as that for Fe.

EPR measurements provide information about the chemical environment of paramagnetic ions in materials. Only one broad EPR signal suggested that the broadening was caused by strong internal magnetic fields. Neighboring metal octahedra in the same crystal contributed to strong internal magnetic fields. When more iron was doped into cryptomelane, the resonance became broader. This may be due to the perturbation caused by Fe^{3+} and the fact that Fe^{3+} has more unpaired electrons (5e) than Mn^{3+} (4e) and Mn^{4+} (3e). The interactions between paramagnetic ions became stronger when more iron was doped into the framework. The *g* value of Fe^{3+} also provided coordination information for the iron in cryptomelane. Fe^{3+} in octahedral sites has a *g* value of 2.0, while Fe^{3+} in tetrahedral sites has a *g* value of 4.2.[17,29,39] The facts that no resonance appeared at the *g* value of 4.2 and the resonance broadened at the *g* value of 2.0 when iron was doped into cryptomelane showed that Fe^{3+} was only in octahedral sites. Because there was no water in cryptomelane, Fe^{3+} could not exist in the form of $Fe(H_2O)_6^{3+}$ in tunnels, in which iron was in octahedral sites. Therefore, Fe^{3+} could only exist in the framework of cryptomelane or as iron oxides.

Iron doping also caused a change in the AOS of manganese in cryptomelane. When the amount of iron doping increased below the doping limit, the AOS of manganese increased at the same time. The AOS of manganese ranged from 3.6 to 3.8, which suggested that both Mn^{3+} and Mn^{4+} existed in cryptomelane and Mn^{4+} was dominant. Because Fe^{3+} has the same charge as Mn^{3+}, Fe^{3+} is more likely to substitute for Mn^{3+} than to substitute for Mn^{4+} though it can substitute for both in the framework. This resulted in less Mn^{3+} relative to Mn^{4+} in the iron-doped cryptomelane framework compared with the case for the undoped cryptomelane, which was reflected in the increase of AOS of manganese (the greater the iron doping, the higher the AOS of manganese). However, the AOS decreased to a number even lower than that for the undoped cryptomelane when the doping was beyond the doping limit. The disruption in the formation of cryptomelane caused by the formation of hematite might have led to a release of some oxygen, resulting in the reduction of some of the Mn^{4+}.

In the cryptomelane tunnel structure, K^+ ions were in tunnels to balance the negative charges of the framework. The substitution of Mn^{3+} by Fe^{3+} did not change the charge of the framework, but the substitution of Mn^{4+} by Fe^{3+} made the framework more negatively charged. More Mn^{4+} ions were substituted if more iron doping was done, resulting in a more negative framework. To balance the charge of the framework, more K^+ was required in the tunnels. This assumption was clearly indicated by the fact that the potassium to metal molar ratio increased as the iron doping increased in cryptomelane.

In the IR spectra, the existence of a C−O stretching vibration was consistent with the thermal analysis results, which indicated that CO_2 was released upon heating. CO_2 must have been adsorbed onto the surface or into the framework of cryptomelane in the preparation process. The band at 700 cm^{-1} was due to the vibration of the metal oxygen bond. Because Fe−O vibration is at 740 cm^{-1}, which is higher than that of Mn−O vibration, 703 cm^{-1},[32,33] the strong interaction of these two vibrations in the framework could cause the upward shift of this metal oxygen vibration band. The continuous upward shift of this band when the Fe to Mn doping ratio was raised suggested that more MnO_6 octahedra were substituted by FeO_6 octahedra in the framework of cryptomelane.

The thermal stability of cryptomelane was improved by iron doping if the doping amount did not exceed the doping limit. Because hematite was more stable than cryptomelane upon heating, doped iron might have helped bind the O_2 absorbed on the surface or in the framework and prevent the release of O_2. The higher thermal stability of doped cryptomelane also delayed the release of CO_2 adsorbed on the surface or in the framework, as shown in the TPD plots of CO_2 of the cryptomelane. However, the TPD plots of CO_2 of the cryptomelane prepared were greatly different from those of CO_2 adsorbed only on basic sites of 700 °C pretreated cryptomelane.

Cryptomelane as prepared had significant amounts of physically adsorbed CO_2 while only chemically adsorbed CO_2 was present in pretreated cryptomelane. This accounts for the larger amount of CO_2 released below 200 °C in the TPD plots of untreated cryptomelane. As for the CO_2 released in the 350−550 °C region, more CO_2 was adsorbed onto the pretreated cryptomelane because high-temperature pretreatment removed species such as O_2 that occupied those strong basic sites. In addition, the amount of CO_2 absorbed by cryptomelane increased with the amount of iron doping under the doping limit, as shown in the TGA profiles. The iron doping might have improved the basicity and, therefore, the CO_2 retentive capability of cryptomelane.

(39) Nam, S. S.; Iton, L. E.; Suib, S. L.; Zhang, Z. *Chem. Mater.* **1989**, *1*, 529.

Conclusions

Iron was doped into the tunnel structure of manganese oxide octahedral molecular sieve cryptomelane using a framework doping method. The doping was achieved by doping iron into the MnO_6 layers of birnessite first, which acted as a synthetic precursor to the tunnel structure cryptomelane, and then by thermally transforming birnessite to cryptomelane. An iron doping limit was observed, and the structure and properties of iron-doped synthetic cryptomelane were studied. Doped iron was found to be in framework sites in synthetic cryptomelane under the doping limit. The AOS of manganese and the thermal stability of cryptomelane increased with the amount of iron doping.

Acknowledgment. We thank the U.S. DOE Office of Basic Energy Science, Division of Chemical Science, for support of this research. We also thank Dr. Harry A. Frank for help with EPR instruments and Dr. Francis S. Galasso for helpful discussions.

CM0014233